

# Representation of a Built-up Area in the Numerical Simulation of Urban Flash Flooding

**Michał Szydłowski**

Gdańsk University of Technology, Faculty of Civil and Environmental Engineering,  
ul. Narutowicza 11/12, 80-952 Gdańsk, Poland, email: mszyd@pg.gda.pl

(Received May 12, 2008; revised June 26, 2008)

## Abstract

The paper concerns numerical simulation of rapidly varied water flow resulting from flash flood propagation in a built-up floodplain. As the mathematical model of free surface unsteady water flow, the shallow water equations are assumed. In order to solve the equations, a numerical scheme of finite volume method is applied. For approximation of mass and momentum fluxes, the Roe method is used. Two methods of built-up area representation in a numerical model are presented in the paper – exclusion of the buildings from the numerical mesh of flow area and substitution of the buildings with high friction zones. In order to assess the quality of the numerical results obtained using both methods, the flow in the model city area with the building group representing a simplified town configuration was simulated. The numerical results were examined against the experimental data available due to laboratory depth measurements. The experiment of model city flooding was carried out in the hydraulic laboratory of Gdańsk University of Technology. Finally, the influence of the type of the boundary conditions imposed on building walls on simulation results is studied.

**Key words:** numerical simulation, flash flooding, urban inundation, built-up area representation, building wall boundary condition

## 1. Introduction

The mathematical modelling of inundations in built-up areas is the main tool for assessment of risks in a city which can be affected by flash flood. The numerical calculations are usually performed to predict and analyze the parameters of catastrophic flow. Then, the predicted flow parameters (water depth and velocity) can be used to estimate the flood influence on city infrastructure and citizens security.

The complexity of mathematical models used by water engineers for modelling of different flood problems varies from one-dimensional Bernoulli steady flow equation, to two-dimensional shallow water flow equations. For urban flash flood modelling, the latter is usually used. There are several techniques that can be applied for representation of buildings in two-dimensional shallow water flow modelling. The choice depends on the ratio of dimensions of flow area and area covered by

the buildings. If the distances between separated buildings are close to the lengths of building walls, the built-up area can simply be excluded from numerical mesh of flow area. In such a case, the building walls form the closed boundaries of the computational domain. However, if the spaces between buildings (streets for example) are significantly smaller than the dimensions of the whole flow area, generation of the proper mesh is often impossible due to high disproportion in mesh elements size inside and outside the built-up area. Therefore, the explicit exclusion of the buildings from the numerical mesh is not possible and they have to be embedded into simulation as the sub-grid effect. The simplest approach consists of representation of built-up areas as zones of reduced hydraulic conductivity. This can be ensured with the high bed friction increasing flow resistance due to the buildings' presence. This technique is often used in water engineering for large scale flood modelling (Szydłowski and Magnuszewski 2007). Another type of urban area representation method is the concept of urban porosity. Shallow water flow equations with porosity were first introduced and implemented in urban flooding simulation by Defina et al (1994) and were later modified by Hervouet et al (2000). Recently this approach for urban flood modelling has been investigated by Guinot and Soares-Fraza (2006) and Soares-Fraza et al (2008). The idea of urban porosity due to the presence of buildings and other structures in the floodplain is similar to the description of flow in a porous medium. In this technique, the permeability of the built-up area has to be defined. The introduction of a porosity concept leads to modified mass and momentum equations in the shallow water flow model. Both methods – increased bottom friction and urban porosity techniques – are usually applied for large scale flood problems providing only averaged characteristics of water flow in a built-up area. Therefore, the local flow effects between buildings are not investigated using these techniques. In this paper, the numerical experiment on urban flash flooding modelling with high friction technique for a small scale problem is presented. The results were examined against measurements and numerical simulations based on buildings exclusion technique.

The buildings representation employing the technique of exclusion of areas covered by buildings' necessitates defining the boundary conditions on the solid buildings walls. Two types of closed boundary conditions can be imposed on the walls in the simulations – no-slip boundaries with zero velocity vector and free-slip boundaries with the normal to the wall component of velocity as well as a derivative of tangential one in the same direction equal to zero. The influence of the condition type on numerical results is investigated in the paper.

## 2. Mathematical Model of Free Surface Water Flow and Solution Method

The flood wave propagation is a three-dimensional time dependent, incompressible, fluid dynamics problem with a free surface. It can be described using Navier-Stokes equations (Prosnak 2006). Unfortunately, due to the complexity data needed to



perform computations and insufficient computer power, this model cannot be applied to simulate the flood inundations in built-up areas. The model most widely used to simulate flood propagation is a system of shallow water equations (SWE). It can be obtained from the Navier-Stokes model using a depth averaging procedure, assuming hydrostatic pressure and uniform velocity distribution along water depth (Szymkiewicz 2000). The SWE model can be presented in conservative form as (Abbott 1979):

$$\frac{\partial \mathbf{U}}{\partial t} + \frac{\partial \mathbf{E}}{\partial x} + \frac{\partial \mathbf{G}}{\partial y} + \mathbf{S} = 0, \quad (1)$$

where

$$\mathbf{U} = \begin{pmatrix} h \\ uh \\ vh \end{pmatrix}, \quad \mathbf{S} = \begin{pmatrix} 0 \\ -gh(S_{ox} - S_{fx}) \\ -gh(S_{oy} - S_{fy}) \end{pmatrix}, \quad (2a, b)$$

$$\mathbf{E} = \begin{pmatrix} uh \\ u^2h + 0.5gh^2 \\ vuh \end{pmatrix}, \quad \mathbf{G} = \begin{pmatrix} vh \\ vuh \\ v^2h + 0.5gh^2 \end{pmatrix}. \quad (2c, d)$$

In the system (1,2)  $h$  represents water depth,  $u$  and  $v$  are the depth-averaged horizontal components of velocity,  $S_{ox}$  and  $S_{oy}$  denote the bed slope terms,  $S_{fx}$  and  $S_{fy}$  are the bottom friction terms, defined by the Manning formula for example, and  $g$  is the acceleration due to gravity. The equation (1) can be presented in another vector form as (LeVeque 2002)

$$\frac{\partial \mathbf{U}}{\partial t} + \nabla \mathbf{F} + \mathbf{S} = 0, \quad (3)$$

where, assuming a unit vector  $\mathbf{n} = (n_x, n_y)^T$ , the vector  $\mathbf{F}$  is defined as  $\mathbf{F}\mathbf{n} = \mathbf{E}n_x + \mathbf{G}n_y$ . In order to integrate the SWE in space using the finite volume method, the domain of solution has to be discretized into a set of cells – triangular for instance (Fig. 1).

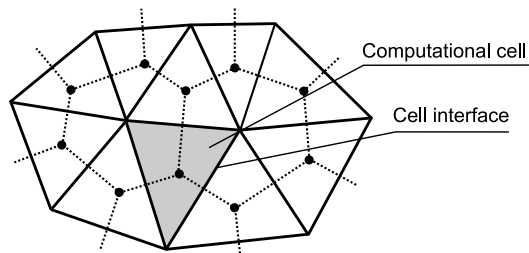


Fig. 1. FVM discretization of the calculation domain



After integration and substitution of integrals by corresponding sums, equation (3) can be rewritten as

$$\frac{\partial \mathbf{U}_i}{\partial t} \Delta A_i + \sum_{r=1}^3 (\mathbf{F}_r \mathbf{n}_r) \Delta L_r + \sum_{r=1}^3 \mathbf{S}_r \Delta A_r = 0, \quad (4)$$

where  $\mathbf{F}_r$  is the numerical flux and  $\Delta L_r$  represents the cell-interface length.  $\mathbf{S}_r$  and  $\Delta A_r$  are the components of source terms and area of cell  $i$  assigned to  $r^{\text{th}}$  cell-interface.

In order to calculate the fluxes  $\mathbf{F}_r$  the Roe (1981) scheme is used. A detailed description of the method is available in the literature (LeVeque 2002, Toro 1997) and is omitted here. For the source term vector  $\mathbf{S}$  computation, the splitting technique with respect to the physical processes is applied. Then, equation (4) is integrated in time using the two-step explicit scheme of finite difference method (Potter 1982). The numerical solution technique was prepared by the author and was tested for numerous simulations of flow in urban areas (Szydłowski 2007).

The model is used here to investigate the influence of the type of buildings-representation technique and the kind of boundary conditions imposed on the buildings' walls on the quality of the numerical simulation results. If the buildings are treated as separate constructions they can be excluded from the calculation domain and the buildings' walls fit exactly with numerical mesh edges. In such a case the walls are solid boundaries of the flow domain, where the proper boundary condition is needed to solve the SWE. Two types of closed boundary conditions can be imposed here – no-slip boundary condition or free-slip condition. Both of them impose the restriction to the normal to the boundary component of the velocity vector  $V_n$ , which has to be equal to zero. If the no-slip boundary condition is imposed, the second velocity component  $V_s$  (tangential to the boundary) is also equal to zero, which is according to the kinematic condition (Sawicki 1998). However, if the free-slip condition is going to be imposed in the numerical solution, the tangential velocity component  $V_s$  has not to be zero, but only its derivative in normal direction to the boundary should be equal to zero. The schematic representation of both types of boundary conditions on the building wall is presented in Fig. 2.

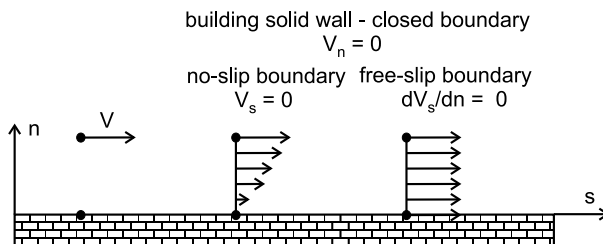


Fig. 2. The types of boundary condition on the building wall



### 3. Laboratory Experiment

In order to carry out the experiment on urban flash flooding, the hydraulic test stand was prepared (Fig. 3). The stand was built in the hydraulic laboratory of Gdańsk University of Technology (Szydłowski 2007).

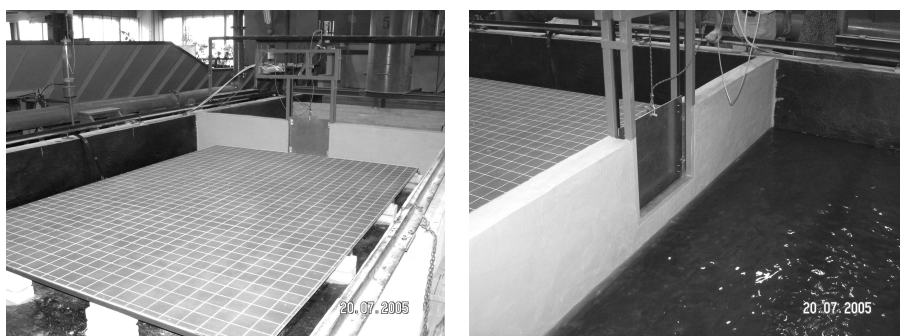


Fig. 3. General view of hydraulic test stand

It is composed of the reservoir (3.0 m length, 3.5 m width) and the horizontal flat plate (3.75 m length, 3.0 m width). The schematic geometry of the flow area is presented in Fig. 4.

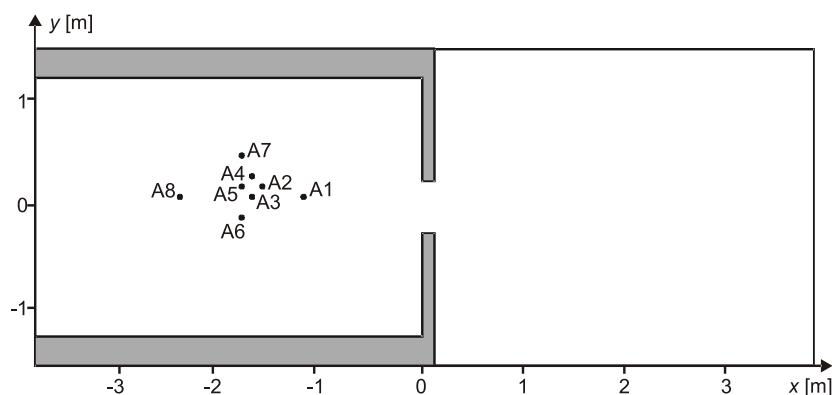


Fig. 4. Geometry of flow area and sensors location

The plate is separated from the reservoir by a solid masonry wall of 0.12 m width. Three other boundaries of the plate are open. The wall contains a 0.5 m wide rectangular breach, which is initially closed by a gate. The gate can be suddenly and fully opened (0.1 s). The gate opening process is automatic. The Manning friction coefficient of the plate and reservoir bottom was estimated as  $n = 0.018 \text{ m}^{-1/3}\text{s}$ .

During experiment the depth variation was measured at several control points shown in Fig. 4. In order to make the measurements, eight pressure sensors were

installed under the plate. The sensors were used to read the water depth at different positions as a function of time. The measurements were recorded and stored using a personal computer (PC). Then, the database of measurements could be used to verify the computation.

In order to simulate the flood in a built-up area, models of buildings were installed on the plate. They were built using cubes of 0.1 m side. A few configurations of building layout were investigated during the laboratory research. In this paper, only one test case is presented – the flow in unstructured buildings-configuration. In this test, the streets have formed a complex system of open channels bounded by the solid walls of model buildings (Figs. 5 and 6).

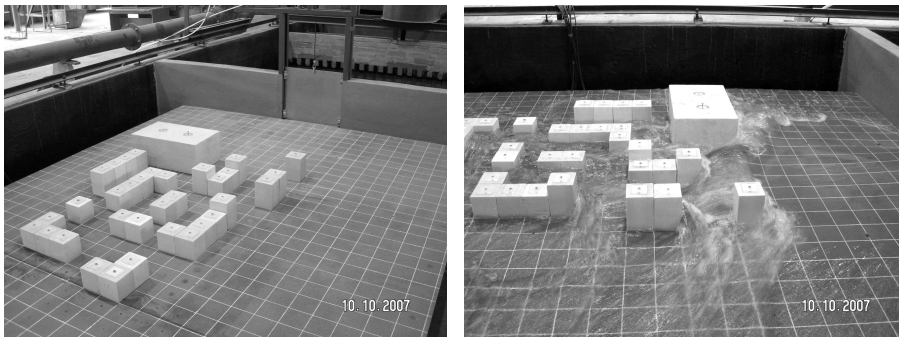


**Fig. 5.** Built-up area configuration and example of flow structure

Initially, there was no water on the built-up plate and the reservoir was filled up to 0.21 m above the plate level. After filling the reservoir with water, the hydrostatic state was achieved using the pipe weir installed in the bottom of the test stand. On opening the gate, the water was released and the built-up plate area was flooded. The experiment was repeated three times and then the time series of water depth variation were averaged. Two tests were investigated: unsteady flow due to reservoir emptying and steady flow with constant reservoir supply, controlled using the weir.

#### 4. Numerical Experiments

First, the unsteady flow in built-up area was simulated excluding the buildings from the calculation domain. In order to carry out this numerical experiment, the calculation domain was covered by an unstructured triangular mesh composed of 13787 computational cells (Fig. 6). The mesh used in the numerical simulation was locally refined between buildings to better represent the complex structure of flow in the city area. The size of computational cells around each building was about 0.02 m, increasing to 0.15 m near the boundaries of flow area.

The boundary conditions were imposed in accordance with experiment. The reservoir walls were treated as closed boundaries. At the open boundaries of the

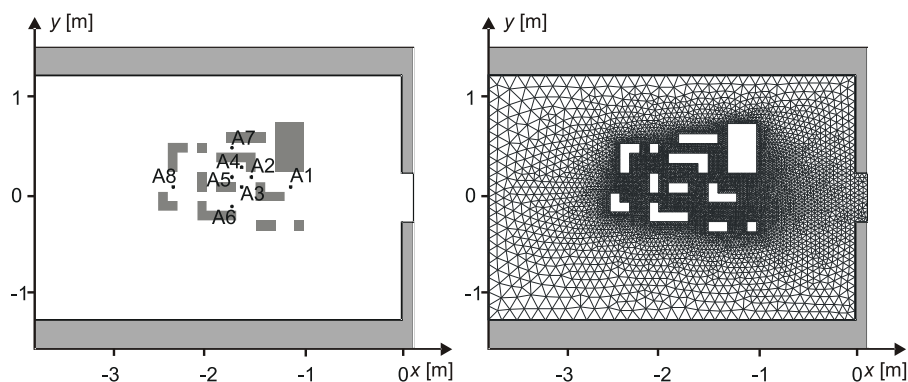


**Fig. 6.** City configuration and part of numerical mesh

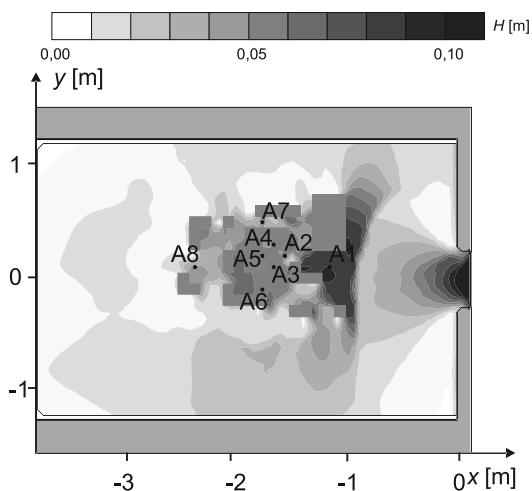


**Fig. 7.** Computed water depth after  $t = 10$  s of simulation (the buildings excluded from flow area)

floodplain the free outflow condition was imposed. The areas occupied by the buildings were excluded from the flow domain, and the free slip boundaries were located at the buildings' edges. The calculation was carried out with the time step  $\Delta t = 0.001$  s. The total simulation time was equal to 20 s.

The flood zone evolution in built-up area can be analysed using results of numerical simulations presented in Figs. 7 and 8. In the former, the example distribution of computed water depth after 10 seconds of numerical simulation is presented. In the latter, the evolution of water depth in time at the control points is presented. After reaching the urban area, the water level swelling can be observed upstream from the first row of buildings. The flood wave reflects there against the buildings resulting in the formation of hydraulic jump. Then, the water flows along the streets. The local water surface swellings can be observed at the corners of buildings' frontages

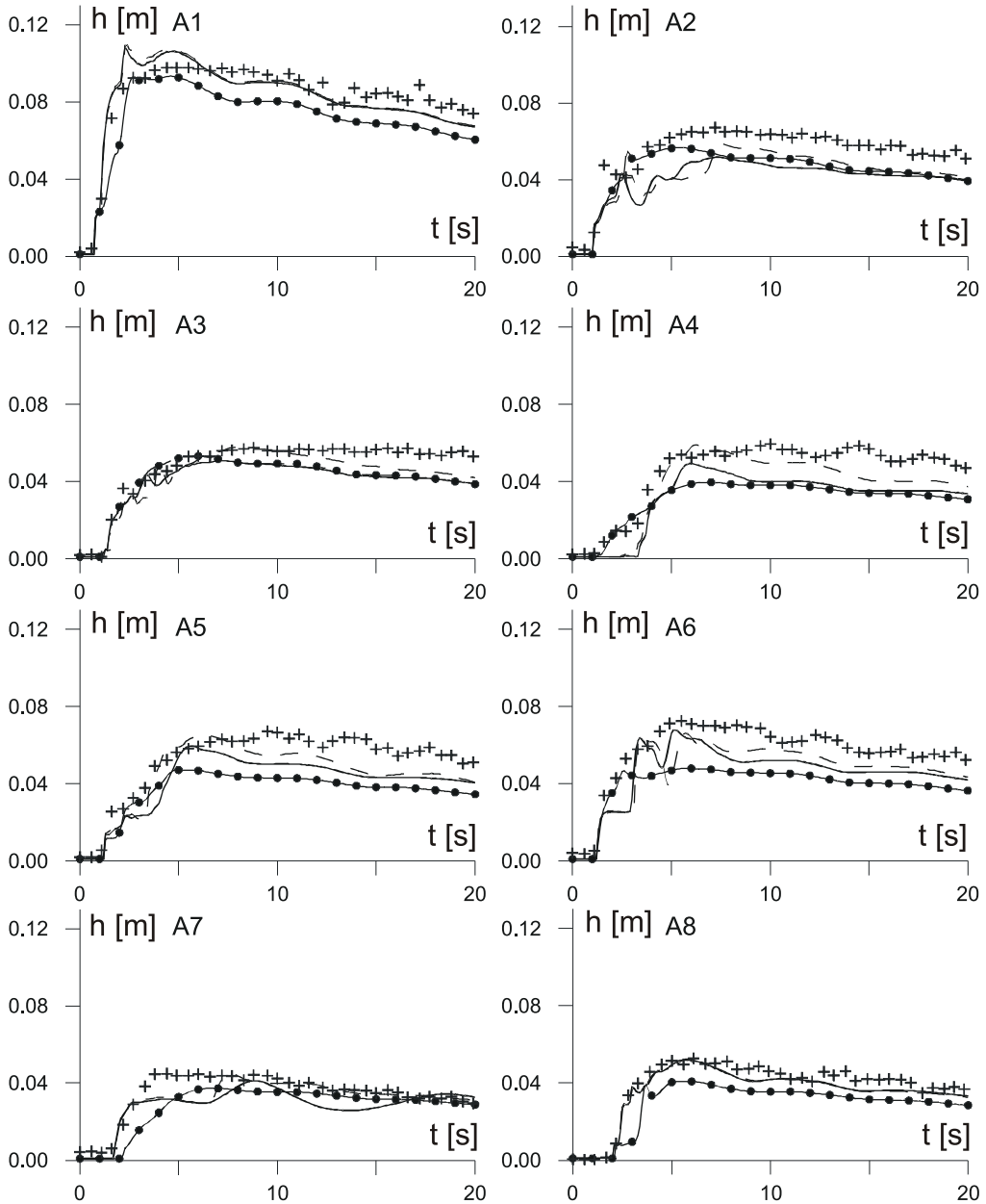


**Fig. 8.** Depth variation at the control points: (++) measured, (—) calculated using buildings exclusion technique and free-slip boundary condition, (●●) calculated using buildings high friction technique, (---) calculated using buildings exclusion technique and no-slip boundary condition





(Fig. 7). The depth decrease, related to the flow acceleration, appears at some cross section constrictions.

The comparison between calculated (solid line) and measured (crosses) depth variations at the control points is shown in Fig. 8. Agreement of the results is satisfactory, however the calculated water depth at the points inside the urban area is generally slightly underestimated. This could be the result of insufficient friction representation in the water flow mathematical model, in which only the bottom friction is incorporated but building walls friction is neglected.

In order to test the technique of high friction representation of buildings in urban areas, the numerical experiment was carried out once again. This time, the buildings were incorporated in the calculation domain but in the built-up areas, the Manning friction coefficient was equal to  $n = 0.5 \text{ m}^{-1/3}\text{s}$ . The flow area was covered by an unstructured triangular mesh composed of 15478 computational cells, filling the flow and buildings areas. The other numerical parameters of the simulation were the same as before.

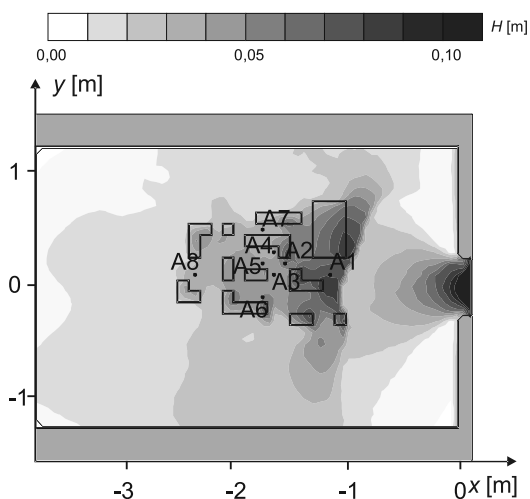


**Fig. 9.** Computed water depth after  $t = 10 \text{ s}$  of simulation (the buildings represented with high friction)

The distribution of computed water depth after 10 seconds of numerical simulation is presented in Fig. 9. Generally, the shape of the water surface outside the buildings is similar to the previously computed one. The swellings can be observed at the front of buildings, however they are shifted downstream. This time, the water is stored in the buildings but the simulated complex flow structure in the streets is realistic, meaning it is comparable to the first calculation carried out with the excluded buildings. The depth variation computed with high friction technique is presented in Fig. 8 (dots). The depth at the control points is underestimated in



relation to the measurements (crosses) and first computation (solid line) as a result of water storage inside the buildings. It can be concluded that generally the results obtained using the high friction technique for buildings representation are in accordance with depth measurements and simulation of flow in built-up area with buildings excluded from the calculation domain. The computed results differ from each other in details but general characteristics of flow in urban areas can be successfully simulated without exact representation of city structure in the numerical mesh.

As mentioned before, when the first calculation was presented, the computed water depth inside the built-up area was underestimated in relation to the observations recorded at the control points. This first simulation was realized with the buildings directly excluded from flow area. Moreover, the free slip boundary condition was imposed on the solid buildings walls. This kind of boundary condition makes the velocity different from zero at the wall. The velocity vector contains here one non zero component – tangential to the wall one.

This kind of solid wall closed boundary condition is usually used in simulation of two dimensional free surface flow, reducing the influence of the wall on the horizontal velocity structure. Considering the flash flow between buildings, it is clear that the influence of walls on the flow should not be neglected. The friction can be observed at the walls' surfaces. The friction reduces the velocity in the vicinity of buildings' walls. In this paper, it is proposed to replace the free-slip boundary condition on the solid buildings' walls with the no-slip boundary condition, which means to reduce the tangential velocity at the wall surface to zero. In order to investigate the influence of the changed boundary condition, the first numerical experiment was repeated once again. All numerical parameters except for the boundary condition were kept as before. The depth variation at the control points computed with no-slip boundary condition imposed in this solution is presented in Fig. 8. It can be seen that for this unsteady flow episode, the computed water depth (dash line) is generally higher than before (solid line) and the agreement with the measurements (crosses) is better for the majority of control points located inside the built-up area.

In order to verify the influence of the kind of boundary condition on the quality of computation, the steady flow experiment was carried out. For the laboratory experiment, the same hydraulic test stand and buildings configuration were used as before. In order to ensure a constant water discharge through the built-up area, the gate was fully open during the experiment. The discharge was controlled by the Thompson weir installed at the reservoir inflow section and was equal to 43.56 l/s. During experiment the depth was measured at the same control points as before. After about 30 seconds from the gate opening, steady flow was observed.

For numerical calculation, the same numerical mesh as in the first simulation was used. The boundary conditions were imposed in accordance with experiment. Two side walls of the reservoir were treated as closed boundaries. Additionally, the



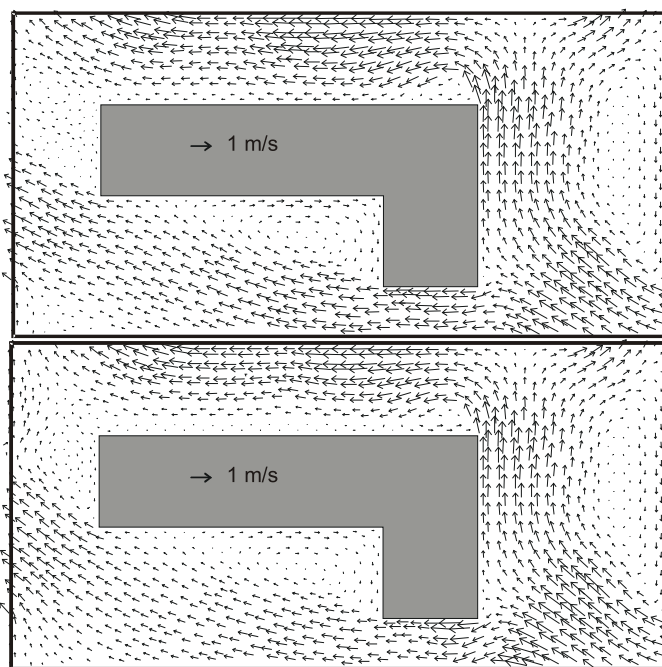


**Fig. 10.** Steady state velocity field around one of the buildings: calculated using free-slip boundary condition (top) and calculated using no-slip boundary condition (bottom)

reservoir was supplied with constant discharge through the inflow section (weir). At the open boundaries of the plate, the free outflow condition was imposed. As the initial condition, the hydrostatic state was assumed. The areas covered with buildings were excluded from the calculation domain. The flow in built-up area was simulated two times. First, calculation was carried out imposing the free-slip boundary condition at the buildings walls, then the no-slip boundary condition was used in the simulation. The calculations were carried out with the time step  $\Delta t = 0.001$  s. The total simulation time was equal to 60 s.

In order to present the influence of the type of solid wall closed boundary condition on the simulation results, the velocity field around one of the buildings is shown in Fig. 10. A difference can be seen between the calculated flow patterns. If the no-slip boundary condition (bottom picture) is used, the velocity near the wall is reduced in relation to the computation with free-slip boundary condition (top picture). In general, the discrepancy in the simulated velocity using both types of boundary condition with decreases distance from the building wall. The velocity decrease is related to the modification of calculated depth. The depth increases in the zones between the buildings. The comparison between depth measurements and results of both calculations for a 30 second period of steady flow is presented in Fig. 11. It can be seen that the depth calculated using the no-slip boundary condition (dash line) better fits the measurements (crosses) for the majority of the

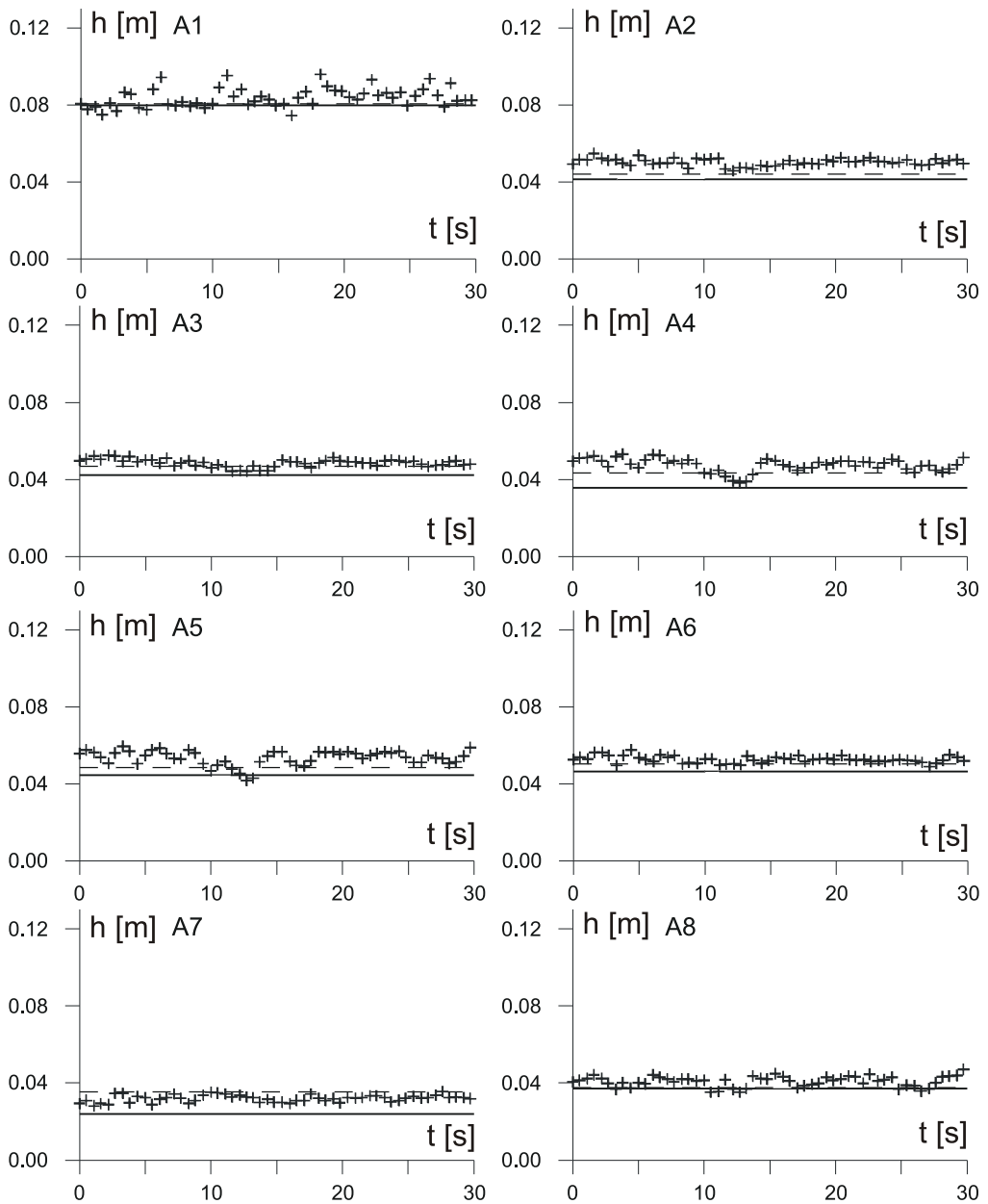


**Fig. 11.** Depth at the control points: (+ +) measured, (—) calculated using free-slip boundary condition, (---) calculated using no-slip boundary condition

control points located between buildings than depth simulated imposing free-slip boundary condition (solid line).

The average values of measured depth are presented alongside calculation results in Table 1. It can be seen that almost all calculated results are underestimated regardless of the type of solid wall closed boundary condition imposed in the simulation. However, the difference between results obtained using no-slip boundary condition and measurements is smaller than for the other kind of boundary condition. Moreover, when the no-slip boundary condition is imposed, the depth discrepancy is close to the measurements deviation.

**Table 1.** Water depth measured and computed at the control points

Control point	A1	A2	A3	A4	A5	A6	A7	A8
measurement $H_m$ [cm]	$8.3 \pm 0.6$	$5.0 \pm 0.2$	$4.8 \pm 0.2$	$4.7 \pm 0.3$	$5.3 \pm 0.3$	$5.2 \pm 0.1$	$3.2 \pm 0.1$	$4.1 \pm 0.2$
calculation using free-slip boundary $H_s$ [cm]	8,0	4.1	4.2	3.6	4.5	4.6	2.4	3.7
$\Delta H_s = H_s - H_m$	-0.3	-0.9	-0.6	-1.1	-0.8	-0.6	-0.8	-0.4
calculation using no-slip boundary $H_c$ [cm]	8.1	4.4	4.7	4.3	4.9	5.0	3.5	3.8
$\Delta H_c = H_c - H_m$	-0.2	-0.6	-0.1	-0.4	-0.4	-0.2	+0.3	-0.3

## 5. Conclusions

The results of preliminary research on the calculation techniques used for building representation in numerical simulation of urban flash flooding was presented in the paper. The following conclusions can be drawn.

1. The shallow water equations can be successfully used for modeling the flash flow in built-up areas.
2. Two techniques of buildings representation were investigated in the research – exclusion of the buildings from flow area and substitution of the buildings with zones of high friction. The former ensures good quality of computational results, verified using the laboratory depth measurements, and provides detailed information about rapidly varied flow structure between buildings. The latter, simplified method of building representation ensures a proper but only a general view of flow in built-up areas. However, it seems that it can be successfully used as well for large and small scale urban flood simulations, simplifying the process of mesh generation in built-up areas. This technique can also be implemented for urban inundation simulation with the effect of water storage inside buildings.
3. If the buildings are excluded from flow area in the flow simulation, two types of boundary condition can be implemented on the closed solid walls – free-slip

boundary or no-slip boundary. When the first kind of boundary condition was imposed in the simulation, a significant underestimation of computed depth was observed for steady and unsteady flow. This could be due to incomplete friction representation in flow modelling. When the second type of boundary condition was used in computation, better results were obtained. It seems that the no-slip boundary condition can approximate wall friction, improving the quality of numerical simulations of flash floods in urban areas.

## References

- Abbott M. B. (1979) *Computational hydraulics: elements of the theory of free-surface flows*, Pitman, London.
- Defina A., D'alpaos L. and Mattichio B. (1994) A new set of equations for very shallow water and partially dry areas suitable to 2D numerical domains, *Proceedings of the special conference, Modeling of flood propagation over initially dry areas*, Milano 29 June–1 July 1994, Italy.
- Guinot V. and Soares-Frazao S. (2006) Flux and source term discretization in two-dimensional shallow water models with porosity on unstructured grids, *International Journal for Numerical Methods in Fluids*, **50**, 309–345.
- Hervouet J. M., Samie R. and Moreau B. (2000) Modeling urban areas in dam-break flood-wave numerical simulations, *Proceedings of RESCDAM Workshop*, Finnish Environment Institute, Seinajoki 1–5 October 2000, Finland.
- LeVeque R. J. (2002) *Finite Volume Method for Hyperbolic Problems*, Cambridge University Press, New York.
- Potter D. (1982) *Computational Physics*, PWN, Warsaw (in Polish).
- Prosnak W. J. (2006) *Equations of Classical Fluid Mechanics*, PWN, Warsaw (in Polish).
- Roe P. L. (1981) Approximate Riemann solvers, parameters vectors and difference schemes, *Journal of Computational Physics*, **43**, 357–372.
- Sawicki J. (1998) *Free Surface Flows*, PWN, Warsaw (in Polish).
- Soares-Frazao S., Lhomme J., Guinot V. and Zech Y. (2008) Two-dimensional shallow-water model with porosity for urban flood modeling, *Journal of Hydraulic Research*, **46** (1), 45–64.
- Szydłowski M. (2007) *Mathematical Modeling of Flood Waves in Urban Areas*, Monographs of Gdańsk University of Technology, **86**, Gdańsk (in Polish).
- Szydłowski M. and Magnuszewski A. (2007), Free surface flow modeling in numerical estimation of flood risk zones: a case study, Gdańsk, *TASK Quarterly*, **11**, 4, 301–313.
- Szymkiewicz R. (2000) *Mathematical Modeling of Open Channel Flows*, PWN, Warsaw (in Polish).
- Toro E. F. (1997) *Riemann Solvers and Numerical Methods for Fluid Dynamics*, Springer-Verlag, Berlin.

